ELSEVIER

Thermochimica Acta 398 (2003) 81–91

thermochimica acta

www.elsevier.com/locate/tca

Chlorination of cerium dioxide

M.R. Esquivel [a,*], A.E. Bohé [b], D.M. Pasquevich [a,b]

[a] *Comisión Nacional de Energía Atómica, Centro Atómico Bariloche, 8400 S.C. de Bariloche, Río Negro, Argentina*

[b] *Comisión Nacional de Energía Atómica, Centro Atómico Bariloche, 8400 S.C. de Bariloche, Río Negro, Argentina*

Received 9 January 2002; received in revised form 29 April 2002; accepted 8 May 2002

Abstract

The chlorination of cerium dioxide was studied by thermogravimetry under controlled atmosphere between 800 and 950 °C. An apparent activation energy of 190 kJ mol^{-1} was observed. To discriminate the effect of the vaporization of the $CeCl_3$ on the chlorination rate, this process was also studied with the same technique between 850 and 950 °C. An apparent activation energy of 184 kJ mol^{-1} was determined. The CeO_2 chlorination rate was found to be under a chemical-mixed control influenced by the vaporization of $CeCl_3$.

Keywords: Ceria; Chlorination; Gas–solid; Thermogravimetry

1. Introduction

Lanthanides occur mainly in nature as fluorocarbonate or phosphate mixtures in minerals such as bastnaesite and monazite [1,2]. Cerium is the most abundant of these elements in either of the named minerals [1,2]. The extraction of this metal or those of the other rare earth from the ore is difficult to accomplish because of the well-known chemical similarities exhibited among lanthanide elements. The production of these metals is based on three well-established methods [2]: (a) the reduction of the anhydrous chloride, (b) the reduction of the oxide and (c) the electrolysis of the fused chloride salt. Methods (a) and (c) require anhydrous rare earth chlorides that can be produced by the chlorination of the respective oxides or lanthanide bearing minerals [2–6].

But unlike those of all light lanthanide sesquioxides (La–Eu), the direct reaction of CeO_2 with Cl_2 is not thermodynamically favored below 1000 °C. For this reason, the CeO_2 chlorination is performed in the presence of a reducing agent such as carbon [2–4]. Nevertheless, the reaction of CeO_2 with chlorine can be achieved up to full conversion of the solid reactant if the gaseous products are continuously removed. The present research is a first approximation to the kinetics of the direct chlorination of CeO_2 since it has not been reported to the best of the authors' knowledge.

The temporal evolution of the reaction was studied by thermogravimetry under controlled atmosphere. The analysis of both reactants and products at different conversion degrees was performed by scanning electron microscopy (SEM), energy dispersive spectroscopy (EDS) and X-ray diffraction (XRD).

* Corresponding author. Present address: Consejo Nacional de Investigaciones Científicas y Técnicas, Centro Atómico Bariloche, 8400 S.C. de Bariloche, Río Negro, Argentina.
Tel.: +54-2944445293; fax: +54-2944445397.
E-mail address: esquivel@cab.cnea.gov.ar (M.R. Esquivel).

0040-6031/03/$ – see front matter
PII: S0040-6031(02)00323-4

Nomenclature

A	solid sample area (m^2)
D	diffusion coefficient ($m^2\,s^{-1}$)
E_a	activation energy ($kJ\,mol^{-1}$)
FW	formula weight ($kg\,mol^{-1}$)
ΔG°	standard Gibbs free energy ($kJ\,mol^{-1}$)
L	characteristic dimension of the sample (m)
m_0	initial mass sample (mg)
Δm	mass variation (mg)
ΔM	balance mass variation (mg)
N	molar flow of chlorine ($mol\,s^{-1}$)
NTP	normal temperature and pressure
P	pressure (kPa)
P_v	vapor pressure (kPa)
ΔP	gradient of partial pressure (kPa)
r	reaction rate ($mol\,s^{-1}$)
r_{chlo}	reaction rate ($mg\,s^{-1}$)
r_{vap}	vaporization rate ($mg\,s^{-1}$)
R	reaction rate (s^{-1})
R_g	gas constant ($m^3\,kPa\,K^{-1}\,mol^{-1}$)
R_{vap}	vaporization rate (s^{-1})
Re	Reynolds number (dimensionless)
Sc	Schmidt number (dimensionless)
t	time (s)
T	absolute temperature (K)
u	flow rate ($m^3\,s^{-1}$)

Greek letters

α_{CeO_2}	CeO_2 reaction degree (dimensionless)
α_{CeCl_3}	$CeCl_3$ reaction degree (dimensionless)
ν	kinematic viscosity ($m^2\,s^{-1}$)

2. Experimental

2.1. Materials

Argon, 99.99% purity (AGA, Argentina) and Cl_2, 99.8% purity (Indupa, Argentina) were the gases used in this study. Solid reactant was CeO_2 powder, 99.9% purity (Alfa-Aesar) with a particle size distribution between 5 and 50 μm as observed by SEM and a BET surface area of $4.065 \pm 0.02\,m^2\,g^{-1}$. CeO_2 structure was verified by comparing the experimental lines with those contained on PDF-1 (1996) using PC Identify program (PW1776) [7].

The starting oxide was heated under flowing Ar at 950 °C to determinate the percentage of hydration or carbonation products on the initial oxide mass [8]. The values found were lower than 0.31 wt.% of the CeO_2 mass. Samples of CeO_2 chlorinated at different reaction degrees were removed and analyzed by XRD and EDS.

Anhydrous $CeCl_3$ was prepared from the reaction of CeO_2 with chlorine and carbon in our laboratory [9]. $CeCl_3$ was identified by XRD [10] and handled within a dry-box to avoid hydration [11].

2.2. Experimental procedure

The progress of the reaction was followed using a thermogravimetric system based on a Cahn electrobalance (Model 2000) adapted for working with corrosive gases. It is described elsewhere [12]. Solid samples between 2 and 20 mg were placed in a quartz crucible connected to the weighing unit by a quartz wire and suspended inside a vertical quartz reactor within an electrical furnace. Non-isothermal measurements were achieved by heating the samples from 20 to 950 °C in both pure Ar and Ar–Cl_2 mixture at $p(Cl_2) = 30.3$ kPa. Isothermal measurements were made by heating the sample at the desired operation temperature and maintaining for an hour to allow temperature stabilization. After that, chlorine was injected into the system and mass changes were measured for total gas flow rates between 2.1 and $7.9\,l\,h^{-1}$ and a constant chlorine partial pressure of 30.3 kPa. The relative error on the calculus of the reaction rates was found to be less than 5% for sample masses of 1 mg.

The reaction products were isolated and handled within a glove-box to avoid hydration.

2.3. Expression of results

Thermogravimetric data were corrected to eliminate apparent mass changes due to both Arquimedes' buoyancy and flow effects. The procedure used to correct these errors in thermogravimetry are detailed elsewhere [12]. For convenience, chlorination mass changes were expressed as fractional oxide mass loss:

$$\alpha_{CeO_2} = -\frac{\Delta M}{m_0(CeO_2)} \quad (1)$$

where α_{CeO_2} is the reaction degree referred to the oxide, ΔM the experimental mass change observed and m_0 the initial CeO_2 mass. Since $\Delta M = \Delta m(CeO_2)$, where Δm is the CeO_2 mass change, Eq. (1) is transformed to

$$\alpha_{CeO_2} = -\frac{\Delta m(CeO_2)}{m_0(CeO_2)} \quad (2)$$

then the reaction rate is calculated as

$$R = \frac{d\alpha_{CeO_2}}{dt} = -\frac{1}{m_0(CeO_2)}\frac{dm}{dt}\ (s^{-1}) \quad (3)$$

and the reaction rate expressed as moles of Cl_2 reacted is

$$r = \frac{dn(Cl_2)}{dt} = \left[\frac{2m_0(CeO_2)}{FW(CeO_2)}\right] R\ (\text{mol}\ Cl_2\ s^{-1}) \quad (4)$$

where $n(Cl_2)$ are the moles of Cl_2 and $FW(CeO_2)$ is the formula weight of CeO_2. The reaction rate expressed as mg $CeCl_3$ produced is

$$r_{chlo} = \frac{Rm_0(CeO_2)\,FW(CeCl_3)}{FW(CeO_2)}\ (\text{mg}\ CeCl_3\ s^{-1}) \quad (5)$$

The kinetics of the chloride vaporization is also studied. So, the relative mass loss corresponding to its vaporization is expressed as

$$\alpha_{CeCl_3} = -\frac{\Delta M}{m_0(CeCl_3)} \quad (6)$$

where α_{CeCl_3} is the cerium chloride vaporization degree expressed as a ratio of the chloride mass loss to the initial chloride mass and ΔM the mass loss observed in the thermobalance. Like the preceding case, $\Delta M = \Delta m(CeCl_3)$. So, Eq. (6) is transformed to

$$\alpha_{CeCl_3} = -\frac{\Delta m(CeCl_3)}{m_0(CeCl_3)} \quad (7)$$

Then, the vaporization rate is calculated as

$$R_{vap} = \frac{d\alpha_{CeCl_3}}{dt} = -\left(\frac{1}{m_0(CeCl_3)}\right)\left(\frac{dm}{dt}\right)\ (s^{-1}) \quad (8)$$

The reaction rate expressed as mg $CeCl_3\ s^{-1}$ is

$$r_{vap} = R_{vap}m_0(CeCl_3)\ (\text{mg}\ CeCl_3\ s^{-1}) \quad (9)$$

3. Results and discussion

3.1. Analysis of the chlorination of CeO_2: reaction products and stoichiometry

The only known and well-determined anhydrous cerium chloride is $CeCl_3$ [11,13]. Although there exists an oxychloride, CeOCl [14], little information is available in the literature about its thermal stability. The theoretical existence of $CeCl_2$ [15] and the possibility of its formation have been discussed since the earlier 1960s [14,16]. No conclusive evidence has been reported and no simple lanthanide tetrachlorides are known [11,14,17]. Nevertheless, exploratory tests were performed to determine the CeO_2 chlorination product. Gases produced in the reaction were condensed, isolated and analyzed by XRD. The most intense lines of $CeCl_3$ corresponding to 2θ equal to 13.675°, 23.843°, 31.658°, 34.66°, 42.507°, 66.33° and 66.31° were identified. These were in agreement with the most intense ones contained in PDF-1 database [10]. No lines corresponding to CeOCl structure were observed [18]. So, the stoichiometry of the chlorination of CeO_2 is represented by the following equation:

$$CeO_2(s) + \tfrac{3}{2}Cl_2(g) = CeCl_3(l) + O_2(g) \quad (I)$$

Since the reaction is studied from 800 to 950 °C, $CeCl_3$ can appear as solid or liquid due to its melting point of 816.9 °C [19]. On this temperature range, $CeCl_3$(l) volatilizes as a monomer [19]. The vapor pressure in equilibrium is described by the following expression [19]:

$$\log P\ (\text{kPa}) = \frac{1634.7}{T} + 2.8203 - 0.6\log(T) \quad (10)$$

3.2. Reactivity of CeO_2 with chlorine

Although the standard Gibbs free energy change (ΔG°) of reaction (I) is positive, viz. $\Delta G^\circ = -2.905 \times 10^{-5}T^2 + 0.406 \times T + 37.18\ \text{kJ mol}\ Cl_2^{-1}$ [20], the formation of $CeCl_3$ is achieved in flowing Cl_2 due to the continuous removal of the reaction products. The CeO_2 mass loss when heated in a Ar–Cl_2 gas mixture is illustrated in Fig. 1A. A significant mass loss is observed above 800 °C. This is due to the vaporization of $CeCl_3$(l) formed according

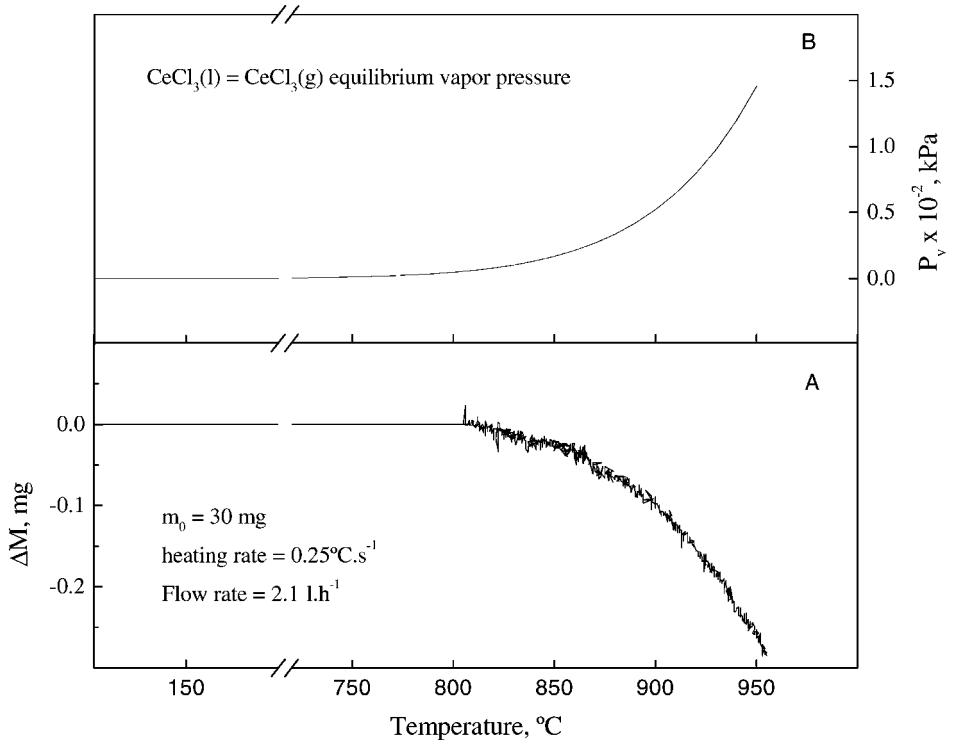

Fig. 1. The non-isothermal TG curve of the chlorination of 30 mg of CeO_2 (A). The equilibrium vapor pressure of the $CeCl_3(l) = CeCl_3(g)$ reaction (B).

to (I). The $CeCl_3(l) = CeCl_3(g)$ vapor pressure equilibrium curve is illustrated in Fig. 1B. Over 800 °C, there is a remarkable raising of the vapor pressure values varying from 4.61×10^{-4} kPa at 800 °C to 1.46×10^{-2} kPa at 950 °C.

3.3. The effect of mass transfer processes on the reaction rate

To determine the intrinsic kinetic parameters of a heterogeneous reaction, the effects of mass transfer should be disregarded first. The reaction rate is influenced by mass transfer when the rate of gas transference through the boundary layer or the gas diffusion rate in the inner pores of the sample are slower or comparable to the chemical reaction rate. However, the mass transference associated to the depletion of the reaction products from the surface should be also analyzed before assuming chemical control rate.

The external mass transference can influence the reaction rate by starvation or convective mass transfer [21]. To analyze starvation, samples of 2 mg were selected. These mass values are small enough to minimize both temperature and concentration gradients of gaseous species. The effect of gas flow rate on the mass loss of CeO_2 at 950 °C is displayed in Fig. 2. The reaction rate is increased when the gas flow rate is incremented from $2.1\,l\,h^{-1}$ (curve a) to $4.55\,l\,h^{-1}$ (curve b). When this parameter is changed from 4.55 to $7.9\,l\,h^{-1}$ (curve c), no further increment on the reaction rate is observed. Therefore, gas starvation is absent at both flow rates higher than $4.55\,l\,h^{-1}$ [21,22] and temperatures lower than 950 °C.

Despite the fact that gas starvation is absent, convective mass transfer can still control the rate of chlorine transference through the boundary layer [21]. It can be estimated from the Ranz–Marshall equation, as described in Appendix A [21,22].

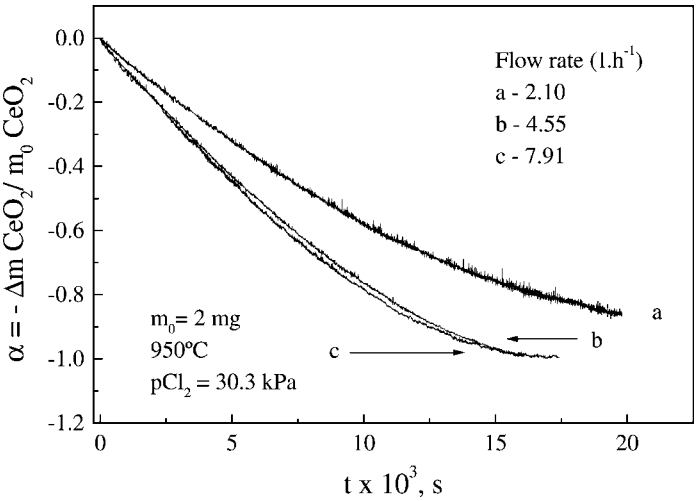

Fig. 2. Effect of the total flow rate of the Cl_2–Ar mixture on the chlorination of CeO_2.

Corrections to the equation, also mentioned in Appendix A, have to be made [22,23]. Corrected values calculated from this equation and those obtained experimentally at $\alpha_{CeO_2} = 0.2$ are shown in Table 1. Parameters D and ν used in calculations are also shown. The values of the reaction rate at different temperatures under various experimental conditions are threefold orders lower than those estimated from the corrected Ranz–Marshall equation. So, since the estimated chlorine gas supply through the boundary layer is three orders faster than the experimental reaction rate, external mass transfer is not a rate-controlling step for gas flow rate values over $4.55\,l\,h^{-1}$.

The next point to be analyzed is the mass transference into the pores of the sample. It is performed by changing the depth and maintaining a constant shape of the solid bed. The procedure is illustrated in Fig. 3 where the relative mass loss of different initial masses of CeO_2 is plotted against time at 950 °C and a total gas flow rate of $7.9\,l\,h^{-1}$. As observed, the relative mass loss rate becomes faster as sample mass is diminished, i.e. the time to reach a fixed reaction degree is higher as the mass sample is increased. To study the effect of the temperature, masses of 2 mg were selected to be both low enough to minimize gaseous product concentration within the pores and reproducible enough in order to maintain

Table 1
Values of D and ν at various temperatures for $p(Cl_2) = 30.3$ kPa. N values are both calculated according to the Ranz–Marshall equation and corrected as explained in Appendix A. In this equation $L = 0.30$. The experimental values of r are obtained at $\alpha = 0.2$ for 2 mg of CeO_2 under a $p(Cl_2) = 30.3$ kPa and a total gas flow rate of $7.9\,l\,h^{-1}$ at each temperature

T (°C)	D ($cm\,s^{-2}$)	ν ($cm\,s^{-2}$)	N ($mol\,Cl_2\,s^{-1}$)	r ($mol\,Cl_2\,s^{-1}$)
800	1.09	0.96	2.62×10^{-7}	1.20×10^{-10}
825	1.13	1.00	2.75×10^{-7}	1.97×10^{-10}
850	1.18	1.04	2.76×10^{-7}	2.96×10^{-10}
875	1.22	1.08	2.77×10^{-7}	6.00×10^{-10}
900	1.27	1.12	2.87×10^{-7}	9.56×10^{-10}
925	1.31	1.16	2.87×10^{-7}	1.05×10^{-9}
950	1.36	1.21	2.88×10^{-7}	1.25×10^{-9}

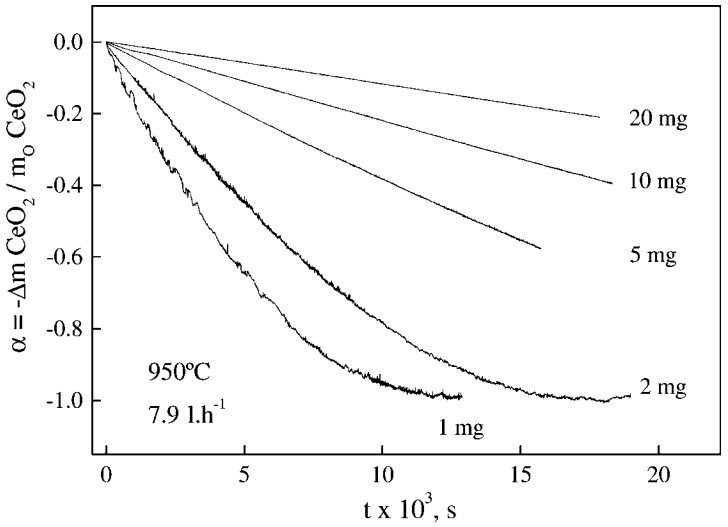

Fig. 3. Effect of the sample mass on the chlorination of CeO_2.

an error on the calculus of the reaction rate below 5% [24].

3.4. The effect of the temperature on the chlorination of CeO_2

The effect of the temperature on the reaction rate was investigated by isothermal TG measurements between 800 and 950 °C. As shown in Fig. 4, the reaction rate is increased as the temperature is raised. For instance, the time to reach $\alpha_{CeO_2} = 0.4$ is 2.3718×10^5, 9836×10^4 and 4.945×10^4 s at 825, 875 and 925 °C, respectively. The straight lines displaying the calculus of the activation energy are shown in Fig. 5 for samples of 2 mg under a chlorine partial pressure of 30.3 kPa and for $\alpha_{CeO_2} = 0.10$, 0.30 and 050. The

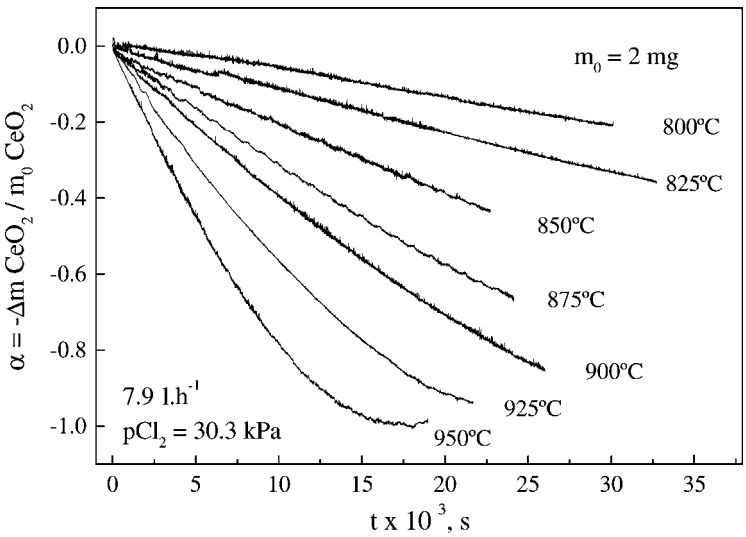

Fig. 4. Effect of the temperature on the chlorination of 2 mg of CeO_2.

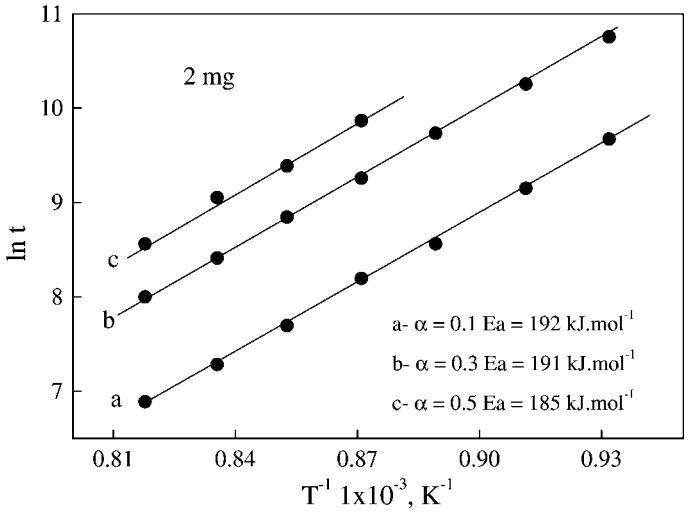

Fig. 5. Plot of $\ln t$ vs. T^{-1} for various conversions of 2 mg of CeO_2.

curves are parallel at all reaction degrees considered. Therefore, the reaction mechanism is the same in all the temperature ranges studied. For convenience, only three lines are shown. But the mean value of E_a found, considering all reactions degrees, is of the order of $190 \pm 8\,kJ\,mol^{-1}$. This high value suggests the presence of a kinetic regime under either chemical or mixed control.

To determine if a decrement of the sample mass produces a change in the controlling regime, the effect of the temperature between 800 and 950 °C was studied for samples of 1 mg at the same experimental conditions to those of 2 mg. The behavior and the activation energy values were similar to those found for 2 mg. Therefore, no change in the reaction regime is observed when the initial mass is decreased twice its value. A further analysis of the characteristics of the CeO_2 chlorination curves is made before assuring that the reaction rate is controlled by a chemical-mixed regime.

A typical TG curve at 875 °C is shown in Fig. 6 for 2 mg of CeO_2 under a chlorine partial pressure of 30.3 kPa and at a total gas flow rate of $7.91\,h^{-1}$. The chlorination evolves with time as a global gasification reaction by loosing mass until all CeO_2 is exhausted. But there are alternatively flat and steeped zones along all the TG curves. A zone showing these features is zoomed out on the right inset of the figure. This behavior is not typical of gasification reactions [22,27,28]. It could not be attributed to artifacts belonging to the TG equipment. The steeped regions of the TG curve are attributed to a rapid vaporization of the produced chloride. The flat ones are thought to be a zone where the rates of liquid formation and vaporization of $CeCl_3$ are competing. That would be probable because the vapor pressure of the chloride is of the order of 1.46×10^{-2} kPa at 950 °C as observed in Fig. 1. These low pressure values would make rather difficult the rapid vaporization of the chloride from the crucible [29]. Then, the kinetics of the chlorination of CeO_2 would be influenced by two processes: a chemical-mixed regime leading to the formation of the chloride and the vaporization of this product. The last one is necessary to free the reactive surface of the oxide to continue the progress of the reaction.

3.5. The effect of the temperature on the vaporization of $CeCl_3$

To discriminate if the direct chlorination rate is influenced by the vaporization of $CeCl_3$, the effect of the temperature on the chloride vaporization in an $Ar–Cl_2$ atmosphere was studied between 850 and 950 °C for anhydrous $CeCl_3$ samples of 2.6 mg. The study was performed for a $Ar–Cl_2$ mixture at a total flow rate

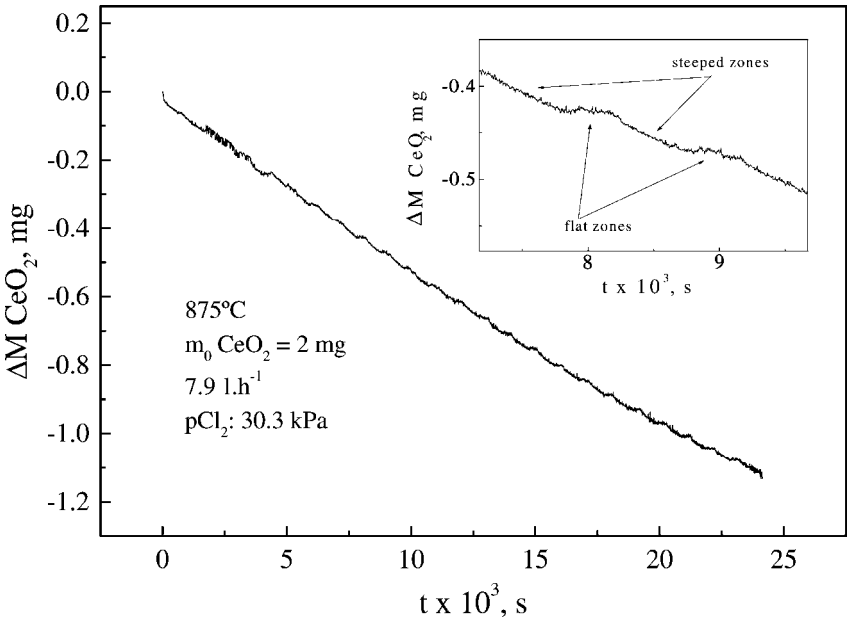

Fig. 6. TG curve at 875 °C. The upper-right inset shows a zoomed zone of the TG curve where the steeped and flat zones are indicated by arrows.

of 7.9 l h^{-1} and under a chlorine partial pressure of 30.3 kPa. The corresponding isothermal TG curves are shown in Fig. 7. As observed, the vaporization rate is increased as temperature is raised, obviously due to the increment on the vapor pressure of the chloride. The presence of an activated process is evidenced. Therefore, the calculation of the activation energy was performed. The resulting lines at various reaction degrees are shown in Fig. 8. The lines are both straight and parallel which means that the vaporization

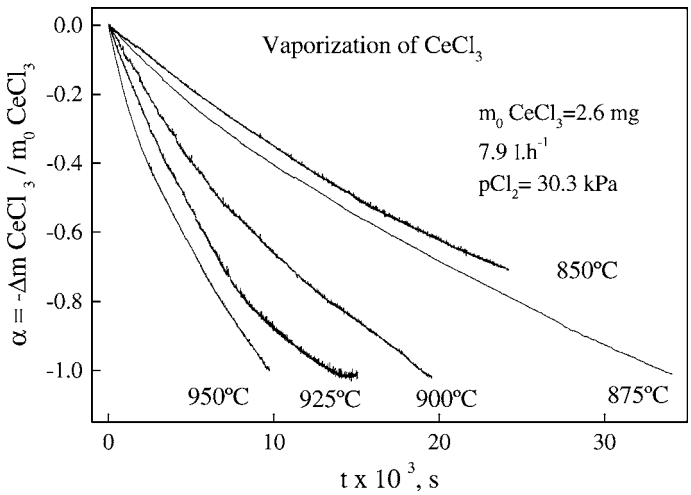

Fig. 7. Effect of the temperature on the vaporization of $CeCl_3$. The isothermal curves are achieved at the same total flow rate and chlorine partial pressure than those of Fig. 4.

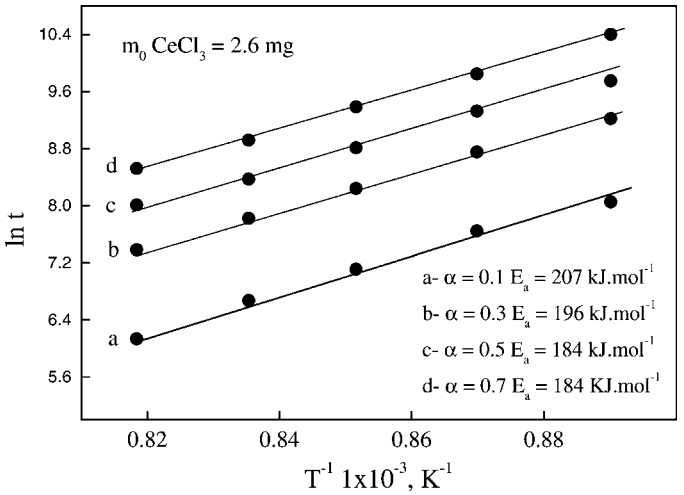

Fig. 8. Plot of $\ln t$ vs. T^{-1} for various conversions of 2.6 mg of $CeCl_3$.

process evolves with the same mechanism at all the reaction degrees and in all the temperature ranges studied. The activation energy values are in the order of $184 \pm 5\,kJ\,mol^{-1}$. But, the theoretical value corresponding to the enthalpy change of the $CeCl_3$ vaporization is of the order of $243\,kJ\,mol^{-1}$ at 950 °C and $306\,kJ\,mol^{-1}$ at 800 °C [20]. This difference can be explained on the basis of the different physical situations involved. The theoretical values are obtained when the system studied is closed and in equilibrium. It is not the case of the analyzed system. The E_a value found for the vaporization process is close to that obtained for the chlorination of 2 mg of CeO_2. The similar activation energy values found only assures that both processes are accelerated by the same ratio. Therefore, no conclusion can be made of the predominance of either of them on the chlorination rate. It is discussed in the next point.

3.6. A comparison of the rates of vaporization of $CeCl_3$ and chlorination of CeO_2

The chlorination of CeO_2 leads to the formation and further vaporization of $CeCl_3$ and the vaporization of $CeCl_3$ evaluates the removal of this product. To discriminate if the second process influences the first one, the rates are compared in Table 2. This table shows the mean experimental $CeCl_3$ vaporization rates obtained at $\alpha_{CeCl_3} = 0.5$ calculated at different temperatures according to Eq. (9) and the mean experimental chlorination rates at $\alpha_{CeO_2} = 0.5$ calculated at the same experimental conditions according to Eq. (5). The rate values are of the same order. No categorical conclusion can be obtained.

An additional discussion is conducted to clarify the point. As already explained, CeO_2 chlorination progresses by the continuous removal of the products. The chloride removal is increased as temperature is raised. But there are two reaction products: $CeCl_3$ and O_2. If either of them were evacuated, the reaction could progress. Since the chloride has very low practical vapor pressures [29] its exit will not be produced until it reaches appreciable vapor pressure values. That is possible at temperatures higher than 800 °C as shown in Fig. 1. O_2 removal is a different matter in nature. The chlorinating agent is Cl_2 with low oxygen level

Table 2
Experimental mean rate values at various temperatures for $p(Cl_2) = 30.3\,kPa$. Both r_{chlo} (Eq. (5)) and r_{vap} (Eq. (9)) are calculated at $\alpha = 0.5$ for 2.6 mg of $CeCl_3$ and 2 mg of CeO_2 at $7.91\,h^{-1}$ at each temperature

T (°C)	r_{chlo} (mg $CeCl_3\,s^{-1}$)	r_{vap} (mg $CeCl_3\,s^{-1}$)
875	6.06×10^{-5}	8.76×10^{-5}
900	8.70×10^{-5}	1.53×10^{-4}
925	1.43×10^{-4}	2.33×10^{-4}
950	2.50×10^{-4}	2.53×10^{-4}

impurities. A simple calculation shows that the O_2 impurities concentration on the Ar–Cl_2 mixture flow are of the order of 4.4×10^{-4} mol l^{-1} at CNPT. This values are high enough to displace the equilibrium of reaction (I) to the left. If O_2 were successfully removed, a mass increment would be shown at temperatures below 800 °C. Instead, the slow mass decrement is shown over 800 °C in the TG isotherms. That is coincident with the remarkable raising in the chloride vapor pressure values. If the vaporization were exclusive rate controlling, a mass gain should be observed during the chlorination and the chlorination curves would at least be as fast as the vaporization ones. As shown in Table 2, it is not the case. So, it can be concluded that the evolution of the chlorination reaction is influenced by both processes according to the following schemes:

$$CeO_2(s) + \tfrac{3}{2}Cl_2(g) = CeCl_3(l) + \tfrac{1}{2}O_2(g) \quad \text{(I)}$$

$$CeCl_3(l) = CeCl_3(v) \quad \text{(II)}$$

4. Conclusions

The chlorination of CeO_2 is not thermodynamically favored. It is slowly accomplished above 800 °C only by removing the reaction products. The reaction system is complex and both chemical and mass transfer processes are involved. The study of both the effect of total gas flow rate and the comparison between the corrected values estimated from the Ranz–Marshall equation led to the conclusion that neither gas starvation nor convective mass transfer influences the reaction rate. The analysis of the activation energy performed to 1 and 2 mg assures the presence of a mixed-chemical control. The study of the effect of temperature on both the chloride vaporization rate and the oxide chlorination rate led to the conclusion that the kinetics of the chlorination process is influenced by both of them. An apparent activation energy of 190 kJ mol^{-1} was obtained for the chlorination and an apparent activation energy of 184 kJ mol^{-1} for the chloride vaporization. A reaction model will be proposed in the forthcoming paper to discriminate and to establish a quantification of the effect of both chemical reaction-mixed regime and chloride vaporization on the CeO_2 chlorination rate.

Appendix A. The use of the Ranz–Marshall equation

The reactive gas supply from the bulk of the gas to the surface of reaction across the boundary layer can be evaluated through the following equation:

$$N = \frac{D(2.0 + 0.6Re^{1/2}\,Sc^{1/2})A\Delta P}{LR_gT} \quad \text{(A.1)}$$

where N is the transference rate of moles of reacting gas per unit solid sample area, $Re = uL/\nu$ and $Sc = \nu/D$ are the Reynolds and Schmidt numbers, respectively. The symbols u, D, L, R_g, T, ΔP and ν stand for flow rate, diffusion coefficient of the reacting gas, characteristic dimension of the sample, gas constant, temperature, pressure gradient and kinematic viscosity, respectively. In this equation, D can be estimated through the Chapman–Enskog correlation [25,26]. Although, Eq. (A.1) has been developed to estimate mass transfer on spheres hanging freely on the fluid [21,22,25], it is accurate enough to be used to estimate mass transfer on thermogravimetric experiences. Corrections have been suggested to approximate mass transference values to the geometry of particles contained in a crucible [21,23]. These corrections consider that the mass transfer to a crucible is one or two orders [23] of magnitude lower than that indicated by Eq. (A.1).

References

[1] J. Morteani, Eur. J. Miner. 3 (1991) 641.
[2] C.K. Gupta, N. Krishnamurthy, Int. Mater. Rev. 37 (5) (1992) 197.
[3] F.R. Hartley, J. Appl. Chem. 2 (1952) 24.
[4] S.L. Stefanyuk, I.S. Morozov, Zh. Prikl. Khim. 38 (4) (1965) 729.
[5] T. Ozaki, K. Murase, K. Machida, G. Adachi, Trans. Inst. Min. Metall. Sect. C 102 (1996) C141.
[6] W. Brugger, E. Greinacher, JOM 19 (1967) 32.
[7] Joint Committee for Powder Diffraction Standards "Powder Diffraction File", International Center for Diffraction Data, Card No. 340394, Swarthmore, PA, 1996.
[8] T. Sato, Thermochim. Acta 148 (1989) 249.
[9] M.R. Esquivel, A.E. Bohé, D.M. Pasquevich, unpublished work.
[10] Joint Committee for Powder Diffraction Standards "Powder Diffraction File", International Center for Diffraction Data, Card No. 120791, Swarthmore, PA, 1996.
[11] S. Cotton, Lanthanides and Actinides, Macmillan, London, 1991, p. 23.

[12] D.M. Pasquevich, A. Caneiro, Thermochim. Acta 156 (1989) 275.
[13] H.A. Eick, Lanthanide and Actinide Halides, Handbook on the Physics and Chemistry of Rare Earths, Vol. 18, North-Holland, Amsterdam, 1994 (Chapter 124).
[14] D. Brown, Halides of the Lanthanides and Actinides, Wiley, London, 1968.
[15] Y.C. Kim, J. Oishi, J. Less Common Met. 65 (1979) 199.
[16] L.F. Drudding, J.D. Corbett, J. Am. Chem. Soc. 83 (1960) 2462.
[17] J.M. Haschke, Halides, Handbook on the Physics and Chemistry of Rare Earths, Vol. 4, North-Holland, Amsterdam, 1979 (Chapter 32).
[18] M. Wolcyrz, L. Kepinski, J. Solid State Chem. 99 (1992) 409.
[19] S. Boghosian, G.N. Papatheodorou, Handbook on the Physics and Chemistry of Rare Earths, Vol. 23, North-Holland, Amsterdam, 1996 (Chapter 157).
[20] A. Roine, Outokumpu HSC Chemistry for Windows, 93001-ORGT, Version 2.0, Outokumpu Research Oy Information Service, Finland, 1994.
[21] A.W. Hills, Metall. Trans. B 9 (1978) 121.
[22] F.C. Gennari, D.M. Pasquevich, Thermochim. Acta 284 (1996) 325.
[23] G. Hakvoort, Thermochim. Acta 233 (1994) 63.
[24] P.K. Gallagher, D.W. Johnson Jr., Thermochim. Acta 6 (1973) 67.
[25] J. Szekely, J.W. Evans, H.Y. Sohn, Gas–Solid Reactions, Academic Press, New York, 1976.
[26] G.H. Geiger, D.R. Poirier, Transport Phenomena in Metallurgy, Addison-Wesley, Reading, MA, 1973.
[27] J.J. Andrade Gamboa, A.E. Bohé, D.M. Pasquevich, Thermochim. Acta 334 (1999) 131.
[28] F.C. Gennari, A.E. Bohé, D.M. Pasquevich, Thermochim. Acta 302 (1997) 53.
[29] H.H. Kellog, Trans. Met. Soc. AIME 236 (1966) 602.